Journal of Hydrology: Regional Studies xxx (xxxx) xxxx

Contents lists available at ScienceDirect

Journal of Hydrology: Regional Studies

journal homepage: www.elsevier.com/locate/ejrh

Spatio-temporal distribution of water availability in Karnali-Mohana Basin, Western Nepal: Climate change impact assessment (Part-B)

Vishnu Prasad Pandey[a,*], Sanita Dhaubanjar[a], Luna Bharati[a], Bhesh Raj Thapa[a,b]

[a] International Water Management Institute (IWMI), Nepal Office, Lalitpur, Nepal
[b] Universal Engineering and Science College, Lalitpur, Nepal

ARTICLE INFO

Keywords:
Climate change
Karnali
Mohana
Water resources
Western Nepal

ABSTRACT

Study region: Karnali-Mohana river basin, Western Nepal.
Study focus: This study aims to project future climate and assess impacts of climate change (CC) on water availability in the Karnali-Mohana (KarMo) basin. Bias-corrected future climate was projected based on ensembles of multiple models selected from a set of 19 regional climate models (RCMs). The impacts on water availability were then assessed by forcing a well calibrated and validated hydrological model with projected future precipitation (P) and temperature (T) for various climatic scenarios.
New hydrological insights for this region: Results showed that future T is projected to increase spatio-temporally with higher rate for the mountain stations in the winter season; whereas future P has no distinct spatio-temporal trend but increase in dry season precipitation for future periods. The projected changes in P, T and evapotranspiration are expected to alter average annual flow at the outlets of the KarMo and its sub-basins, albeit with varying rate. The simulated results showed higher impacts in water availabilty at higher altitudes, thus indicating higher vulnerability of northern mountainous region to CC than the southern flatlands. Being the first ever study of such nature in the study area, these results will be useful for planning and development of climate-resilient water development projects in the region.

1. Introduction

Climate change (CC) is projected to impact availability and quality of water in future (IPCC, 2014). Climate change alters the timing and intensity of rainfall, temperature, and runoff; challenges coping capacities of existing infrastructures; and brings higher risk of drought and floods, which ultimately affects the hydrological cycle, locally and globally (Kundzewicz et al., 2009; Zhu and Ringler, 2012). The impacts will be further aggravated by demographic, economic, environmental, social, and technological activities (UN-WWAP, 2015). Understanding the extent and significance of CC-induced alterations in the hydrological cycle and subsequent water availability is of a great interest to environment and water resources managers globally (Bates et al., 2008; Honti et al., 2014). Several studies are being carried out at global, local and regional scales to understand water availability under CC (Abbaspour et al., 2009; Aryal et al., 2018; Bharati et al., 2016; Devkota and Gyawali, 2015; Pandey et al., 2019; Shrestha et al., 2016; Trang et al., 2017). However, many local basins such as Karnali-Mohana (KarMo) in Western Nepal (Fig. 1) still lack such studies.

* Corresponding author.
E-mail address: v.pandey@cgiar.org (V.P. Pandey).

https://doi.org/10.1016/j.ejrh.2020.100691
Received 4 December 2019; Received in revised form 7 April 2020; Accepted 20 April 2020

Please cite this article as: Vishnu Prasad Pandey, et al., Journal of Hydrology: Regional Studies, https://doi.org/10.1016/j.ejrh.2020.100691

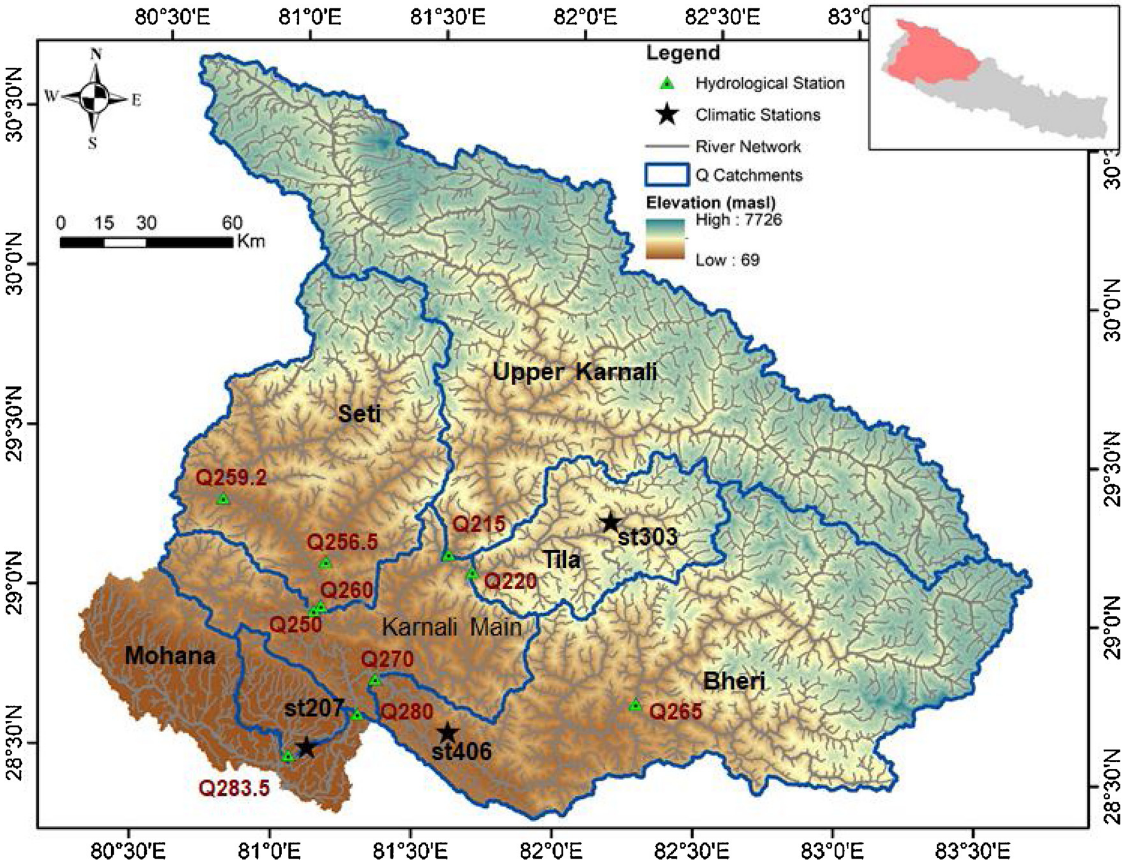

Fig. 1. Location, topographic details, and hydrological stations of the Karnali-Mohana (KarMo) basin. Q-catchments are catchments above the gauging stations.

The KarMo basin in the region covers the area of 49,892 km^2 above Nepal-India border, of which 6.9 % falls in the Tibetan Plateau, China and the rest in Western Nepal, as elaborated in Pandey et al. (2020) (Part-A of this paper). The watershed area of Mohana alone is 3730 km^2. The Karnali river originates in the Trans-Himalayas (TrH) and flows through Mountains (Mnt), Hills (Hil), and Indo-Gangetic Plain (IGP) (Annex-1). The KarMo basin offers large fertile lands for agriculture. In addition, steep slopes, with topographical variations from 69 to 7,726 m above mean sea level (masl), and meandering rivers further offer tremendous potential for hydropower development. Water resources development activities in the KarMo basin are expected to accelerate in future given the country's focus on harnessing water as resource and the potential the KarMo basin has for that. Alterations in streamflow and hydrology induced by CC may affect availability of water for irrigation and hydropower production and then impacts food production, energy generation, and provincial and national economies. Therefore, understanding implications of projected change in climate on spatio-temporal distribution in water availability provides a useful knowledgebase for the policy/decision-makers to quantify different types of water security threats; design policies and programmes; and devise strategies for better allocation, utilization, and management of freshwater resources for the country's prosperity.

There are several studies focusing on hydrological modelling and CC impacts assessments at both local and watershed scales in Nepal (Bajracharya et al., 2018; Bharati et al., 2014; Dhami et al., 2019; Pandey et al., 2019); however none are focused in the KarMo basin. The Western Nepal is mostly susceptible to drought, flood, and climate shocks with increasing magnitude and frequency in the recent years (WECS, 2011). In addition, increase in extreme precipitation events in western mountains are observed in recent decades (Talchabhadel et al., 2018), which could impact aversely to the hydrological cycle and water availability, and then hydropower and agriculture sectors, among others.

A typical CC impact study exploring the hydrological perspective requires time series of projected meteorological variables (at minimum, precipitation and temperature) representing future climate and a well calibrated and validated hydrological model. Future climate projections can be obtained from global circulation models (GCMs) and regional climate models (RCMs). For local-scale basins such as KarMo, projections from RCMs are considered better than that from GCMs. However, RCM projections are not free of biases due to coarse spatial resolution, and therefore need bias-correction before using for local scale CC impact assessments (Maraun, 2014; Teutschbein and Seibert, 2010). Statistical techniques such as empirical quantile mapping (QM) (Maraun, 2014) are used for correcting the biases (Berg et al., 2012; Shrestha et al., 2017; Pandey et al., 2019). Additionally, to reduce uncertainties in the projections, bias-corrected RCM outputs are combined into ensembles representing various climate models as described in

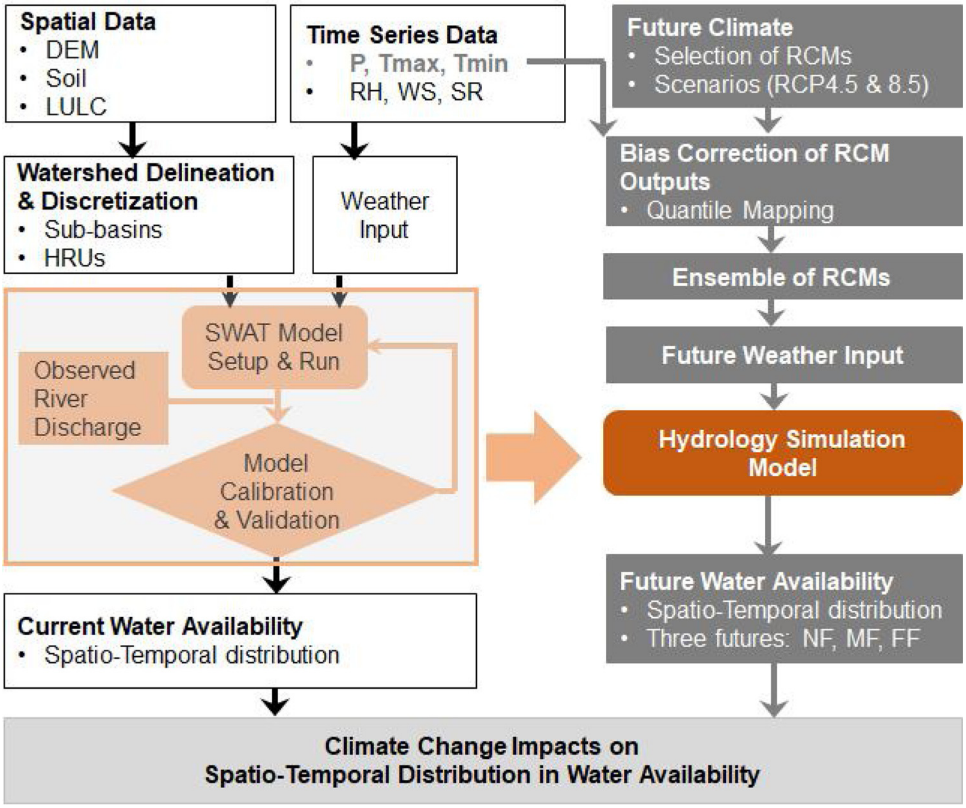

Fig. 2. Methodological framework for assessing climate change impacts on water availability in the Karnali-Mohana (KarMo) basin using a SWAT model. NF, MF, and FF refer to Near-, Mid-, and Far-Futures, respectively; DEM is Digital Elevation Model, LULC is land use/cover; HRU is hydrological response unit.

Dhaubanjar et al. (2018). Ensemble time series are fed to hydrological model for CC impact assessment (Aryal et al., 2018; Tuetschbein and Seibert, 2012).

Climate change impacts on hydrology and water resources availability are generally assessed by forcing a well calibrated and validated hydrological model with bias-corrected RCM outputs under different future scenarios (Bastola et al., 2011). A well calibrated and validated hydrological model in Soil and Water Assessment Tool (SWAT) (Arnold et al., 1998) is already developed for the KarMo basin by Pandey et al. (2020). This study therefore uses that model to assess CC impacts on spatio-temporal distribution in water availability in the basin under current and future conditions for the most recent representative concentration pathways (RCP) scenarios from multiple RCMs. During the process, it also characterizes future climate in the study basin using multi-RCM approach.

2. Methodology and data

This study adopts a model-based approach to assess impacts of projected future climate on spatio-temporal distribution of water availability in the KarMo basin. Fig. 2 depicts a flowchart of adopted methodology and following sub-sections describes them in detail. Future climate were projected using multiple RCMs. Current and future water availabilities were assessed using a hydrological model developed in SWAT.

2.1. Hydrological model

We used the SWAT (Arnold et al., 1998) hydrological model developed by Pandey et al. (2020) (Part-A of this paper) by discretizing the KarMo basin into 111 sub-basins and 2122 Hydrologic Response Units (HRUs). The model was calibrated and validated at 10 hydrological stations along five tributaries of the KarMo (Fig. 1).

2.2. Future climate projection

Nineteen RCMs available in COordinated Regional Downscaling EXperiment for South Asia (CORDEX-SA) platform were evaluated as discussed in Dhaubanjar et al. (2019). The study first compared the annual projections for the northern Mountains, mid Hills and southern Terai regions in Western Nepal from the 19 RCMs using the Australian Climate Futures Framework (Clarke et al., 2011;

Whetton et al., 2012). For each region, projected changes in annual temperature and precipitation were classified into qualitative categories of changes to generate a *climate future matrix*. Three future periods were investigated: near-future (NF; 2021–2045), mid-future (MF; 2046–2070), and far-future (FF; 2071–2095). Considering two RCPs (RCP 4.5 and 8.5) and three future periods, six climate future matrices were developed representing six climate scenarios in each region. From the 18 matrices (6 scenarios x 3 regions = 18 matrices), the RCMs that represent the consensus case (i.e., the matrix category that majority of the RCMs project) were identified and selected.

The future climate data at the meteorological stations were then bias-corrected using quantile mapping (QM) method (Gudmundsson et al., 2012; Teutchbein and Seibert, 2012), implemented in R using a qmap package (Gudmundsson et al., 2012). QM corrects quantiles of RCM data to match with that of observed ones by creating suitable transfer functions. The bias corrected times series from the selected RCMs for each station were averaged to create a multi-model averaged ensemble for each climate scenario. The projected future CC and associated impacts were analysed based on those ensembles.

2.3. Climate change impacts assessment

Bias-corrected precipitation and temperature ensemble projections for six climate scenarios (2 RCPs and three future periods) at the meteorological stations were fed into the calibrated and validated SWAT model developed by Pandey et al. (2020). The simulated streamflows were then characterized in terms of average annual and seasonal values for the three future periods. The deviation of streamflow (annual and seasonal) with respect to baseline (1980–2005) were considered as impact of projected CC on water availability. Similarly, impact of CC in other water balance components such as precipitation and actual evapotranspiration were also assessed as deviation of future values with respect to baseline, using similar approach as used for streamflows. The spatial distribution of change in key water balance components compared to baseline in each sub-basin were explored through spatial maps.

2.4. Data and sources

The data used in hydrological modelling are reported in Pandey et al. (2019). Daily precipitation data at 36 stations, temperature data at 16 stations, relative humidity data at 15 stations, sunshine hours data at 5 stations, and wind speed data at 7 stations were collected from the Department of Hydrology and Meteorology (DHM), the Government of Nepal. Future time series of precipitation (mm) and temperature (°C) data projected by 19 RCMs were extracted from spatial grids of 0.44° x 0.44° (1981–2100) as detailed in Dhaubanjar et a. (2019).

3. Projected future climate

Given the large size of the KarMo, one certainly expects spatial heterogeneity in the projected future climate. To reflect that, future climate at three representative stations spread across the three physiological regions are analysed. The stations are st303 (region = Mountain; elevation = 2300 masl; sub-basin = Tila); st406 (region = Hill; elevation = 720 masl; sub-basin = Thuli Bheri); and st207 (region = Terai in IGB; elevation = 140 masl; sub-basin = Mohana). The station locations are shown in Fig. 1. All changes are reported with respective to average of 1980–2005, as the climatic baseline. The spatio-temporal distribution in the projected precipitation and temperature across the three stations are provided in Figs. 3 and 4, respectively and their ranges are tabulated in Annex-2 and Annex-3.

At a ***mountain*** station-303, average annual precipitation (P) for RCP4.5 (RCP8.5) scenarios are projected to increase by 4% (7%), 10 % (10 %) and 13 % (17 %) in NF, MF, and FF, respectively; however, with variation in rate of change across the seasons (Fig. 3). The rate of change in P varies across the seasons with the highest amount of increase as well as range of projection for ON season for all the future periods and climate scenarios considered, thus, indicating wetter future. In terms of temperature, average annual maximum temperature (Tmax) for RCP4.5 (RCP8.5) scenarios are projected to increase by 1.3 °C (1.3 °C) in NF, 2.3 °C (2.7 °C) in MF, and 2.5 °C (4.5 °C) in FF (Fig. 4). A higher increase is projected for DJF and MAM seasons, which in DJF is 1.6 °C (1.7 °C) in NF, 2.8 °C (3.6 °C) in MF and 3.2 °C (5.9 °C) in FF under RCP4.5 (RCP8.5) scenarios (Fig. 4). The average annual minimum temperature (Tmin) under RCP4.5 (RCP8.5) scenarios as reported in Dhaubanjar et al. (2019), on the other hand, is projected to increase by 1.0 °C (1.1 °C) in NF, 1.7 °C (2.3 °C) in MF, and 1.8 °C (3.9 °C) in FF albeit with higher increase in MAM and ON seasons.

At a ***hill*** station-406, average annual P under RCP4.5 (RCP8.5) scenarios are projected to increase by 5% (8%), 9% (11 %), and 11 % (13 %) in NF, MF, and FF, respectively, with projection ranges as shown in Fig. 3. With higher increase projected for MAM and ON seasons, there exists seasonality in amount and ranges of change in P. In terms of temperature, average annual Tmax under RCP4.5 is projected to increase by 0.9 °C, 1.2 °C, and 1.9 °C in NF, MF, and FF, respectively (Fig. 4). For both the scenarios (RCP4.5 and 8.5), higher increase in Tmax is projected for DJF and MAM seasons, reflecting warmer winters in future. The average annual Tmin, as discussed in Dhaubanjar et al. (2019), is also projected to increase by 1.8 °C, 2.7 °C, and 3.9 °C during NF, MF, and FF, respectively, under RCP4.5 with changes varying across the seasons.

In case of a ***Tarai*** station-207, the P for RCP4.5 (RCP8.5) scenarios are projected to increase by 5% (9%) in NF, 7% (9%) in MF and 6% (6%) in FF (Fig. 3). There is no distinct trend towards the future. In terms of seasons, P is projected to increase in all the seasons, however, with more increase for ON and MAM than others seasons for both the scenarios and all the future considered. Average annual Tmax for RCP4.5 (RCP8.5) scenarios are projected to increase by 1.0 °C (1.2 °C) in NF, 1.3 °C (2.1 °C) in MF, and 1.2 °C (3.3 °C) in FF (Fig. 4). All the seasons project increase in Tmax, however, higher amount of increase is projected for DJF and MAM seasons. In case of Tmin, annual averages under RCP4.5 (RCP8.5) scenarios are projected to increase by 1.2 °C (1.5 °C) in NF, 1.7 °C

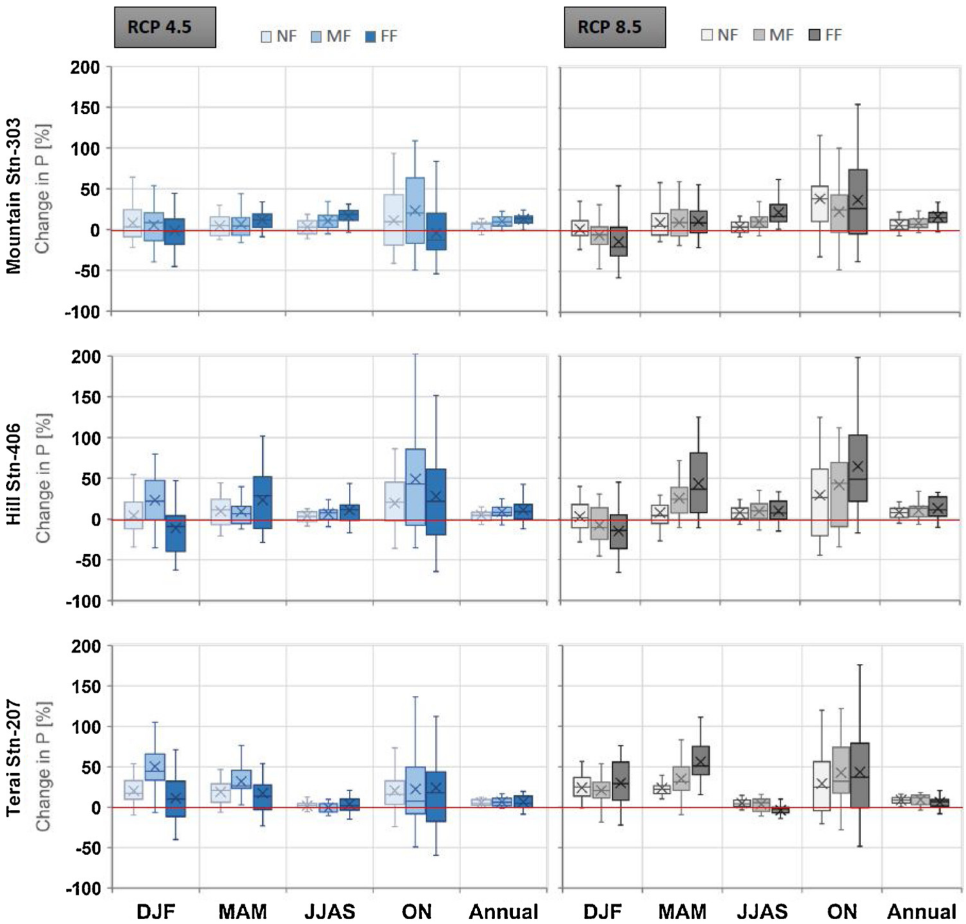

Fig. 3. Spatio-temporal distribution in projected change in precipitation. NF, MF and FF refer to Near-, Mid-, and Far-Futures, respectively. Each box represents range in each season, whiskers indicate max and min values excluding the outliers, '-' marker indicate median, and 'x' marker indicate mean; DJF, MAM, JJAS and ON refer to winter, pre-monsoon, rainy; and post-monsoon seasons, respectively.

(2.8 °C) in MF, and 1.8 °C (4.4 °C) in FF. The MAM and ON seasons are projected to have higher increase in Tmin compared to other seasons as well as annual averages.

Across the three stations, the projection ranges for annual as well as seasonal changes in precipitation and maximum temperature are increasing in general – though not consistent for all the stations, seasons, and scenarios – when we move farther into the future years. It indicates increase in uncertainty in the projection when moved farther in the future. The annual projections for temperature and precipitation seen here are comparable to the ranges reported in Lutz et al. (2016); Sanjay et al. (2017) and Choudhary and Dimri (2018) for the greater Hindu Kush Himalayas. However, seasonal ranges not reported explicitly in most of the studies vary, especially for precipitation. Local orographic effects affect seasonal changes in climate more than annual averages. Variation across the Mountain, Hill and Tarai in Figs. 3 and 4 are likely due to heterogeneity in local conditions and microclimates. Furthermore, given the larger size of the basin, global warming phenomenon might also have contributed to change sin both precipitation and temperature in the entire basin.

4. Climate change impacts on water availability

Projected future temperature and rainfall time series based on an ensemble of the selected RCMs for six consensus scenarios were used as input to the calibrated and validated SWAT model to simulate the CC impacts on future water balance components. Changes in water balance components over the sub-basins as well as months/season were analyzed to understand spatio-temporal distribution of the changes under projected future climates. Since observed data of different water balance components are not available for the basin, output from the SWAT model was used as the baseline to compare with future scenarios.

The sub-basin wide distribution in the change of water balance components, namely, precipitation (P), actual evapotranspiration (AET), and net water yield, for two RCPs (4.5 and 8.5) and three future periods (NF, MF, and FF) are shown in the Figs. 5 and 6. As seen in the plots for station-406 (Figs. 3–4), average annual P is projected to increase gradually from NF to FF. The rate of projected change, however, varies widely across the sub-basins extending beyond +/- 25 % (Fig. 5). Change in P as well as temperature (T) has

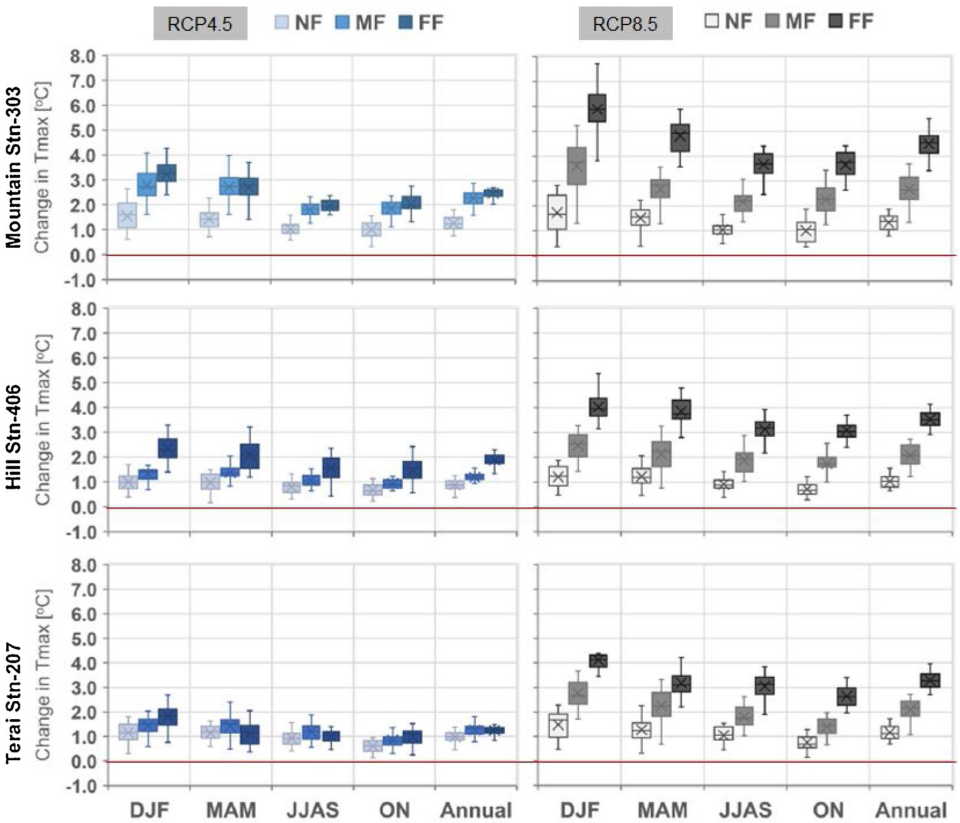

Fig. 4. Spatio-temporal distribution in projected change in maximum temperature. NF, MF and FF refer to Near-, Mid-, and Far-Futures, respectively. Each box represents range in each season, whiskers indicate max and min values excluding the outliers, '-' marker indicate median, and 'x' marker indicate mean.

altered AET from baseline value by varying rates across the sub-basins as shown in Fig. 6. The sub-basin wide AET varies from less than -15 % to above 50 % under the six future scenarios considered. The change in AET is more pronounced at the sub-basins in higher and middle elevations than at the lower elevations, potentially due to higher rate of increase in T in these regions. Similar results are reported for the Koshi basin in Nepal as well (Bharati et al., 2014).

The percentages of sub-basins that show increase and decrease in P, AET, and Q are reported in Table 1. For example, the percentages of sub-basins that show increase (decrease) in P by more than 10 % under RCP4.5 are 10 % (15 %) in NF, 26 % (12 %) in MF, and 32 % (12 %) in FF, under bot the RCP scenarios (Table 1). Similarly, the percentages of the sub-basins that show increase (decrease) in AET by more than 10 % under the RCP4.5 scenarios are 51 % (3%) in NF, 51 % (3%) in MF, and 51 % (4%) in FF. Similar results for RCP8.5 are reported in Table 1.

As a result of changes in P and AET, average annual flow at outlets of the KarMo sub-basins are projected to alter as shown in Fig. 7. In comparison to temperature and precipitation, other input variables such as radiation, relative humidity, and wind speed have a less significant effect on water yield (Stonefelt et al., 2000). The Fig. 7 shows variation in projected changes in average annual flows under RCP4.5 and 8.5 scenarios for the three future periods considered (i.e., NF, MF, and FF). The spatial variation in the change in average annual flow also follows similar pattern as future P, however, the variations across the sub-basins fluctuate a lot. The impacts in the sub-basins at higher altitudes are relatively higher perhaps due to melting of snow/glaciers as a result in change in T. This indicates that high mountain regions are more vulnerable to CC than the flatlands in the lower part of the basin. For example, under RCP4.5 scenarios, the regional average net water yield in NF for IGP, Hil, Mnt, Mnt and TrH are projected to change by 8.3 %, -0.2 %, -2.8 % and -5.6 %, respectively.

4.1. Bheri river basin

The Bheri river basin above the Q270 hydrological station has a catchment area of 12,290 km^2. The average annual flow volume at Q270 for the baseline period is estimated at 11,383 MCM, which under RCP4.5 scenarios are projected to decrease in NF by -5.4 % and then increase in MF by 3%. Under RCP8.5 scenarios, it is projected to decrease by -2.5 % and -1.3 % for NF and MF, respectively. However, intra-annual variations of the projected changes vary across the scenarios and future periods considered. Projected changes under both the scenarios vary from -30.5 % (May) to 11.7 % (January) in NF, -28.5 % (May) to 26.2 % (January) in MF, and -28.5 % (May) to 13.4 % (January) in FF. While moving towards farter in the future, the flow volume in the Bheri river is projected to

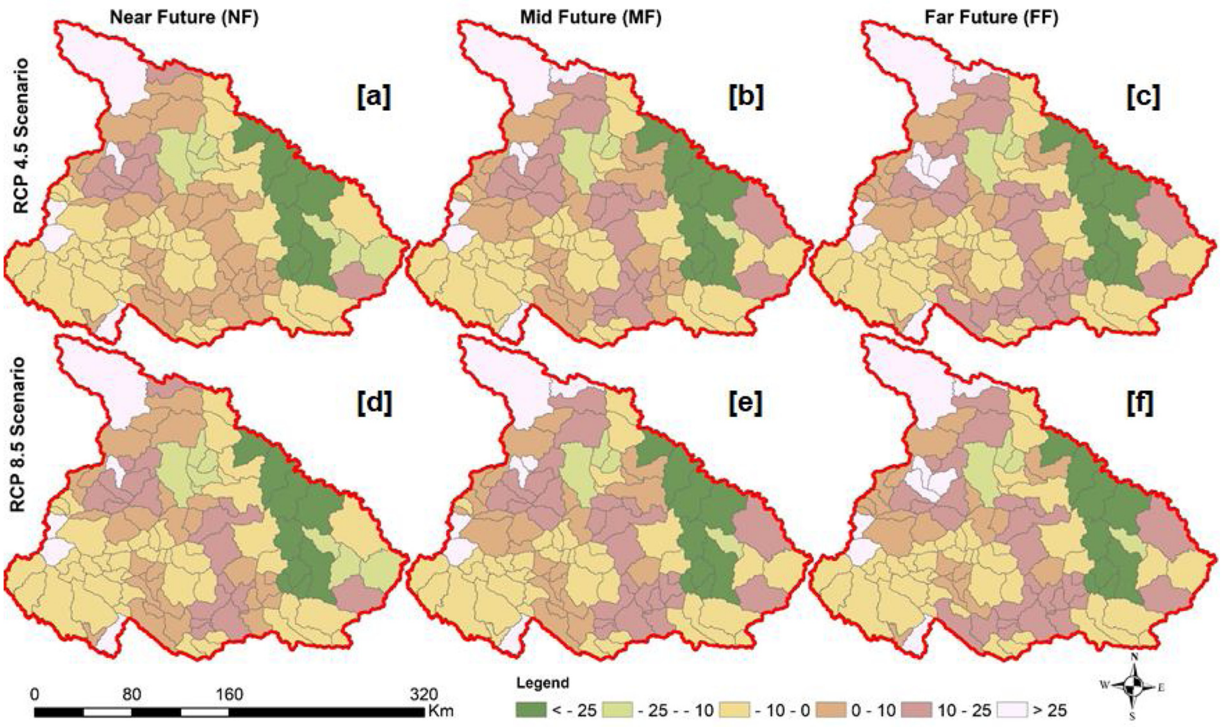

Fig. 5. Change (%) in average annual precipitation with respect to the baseline.

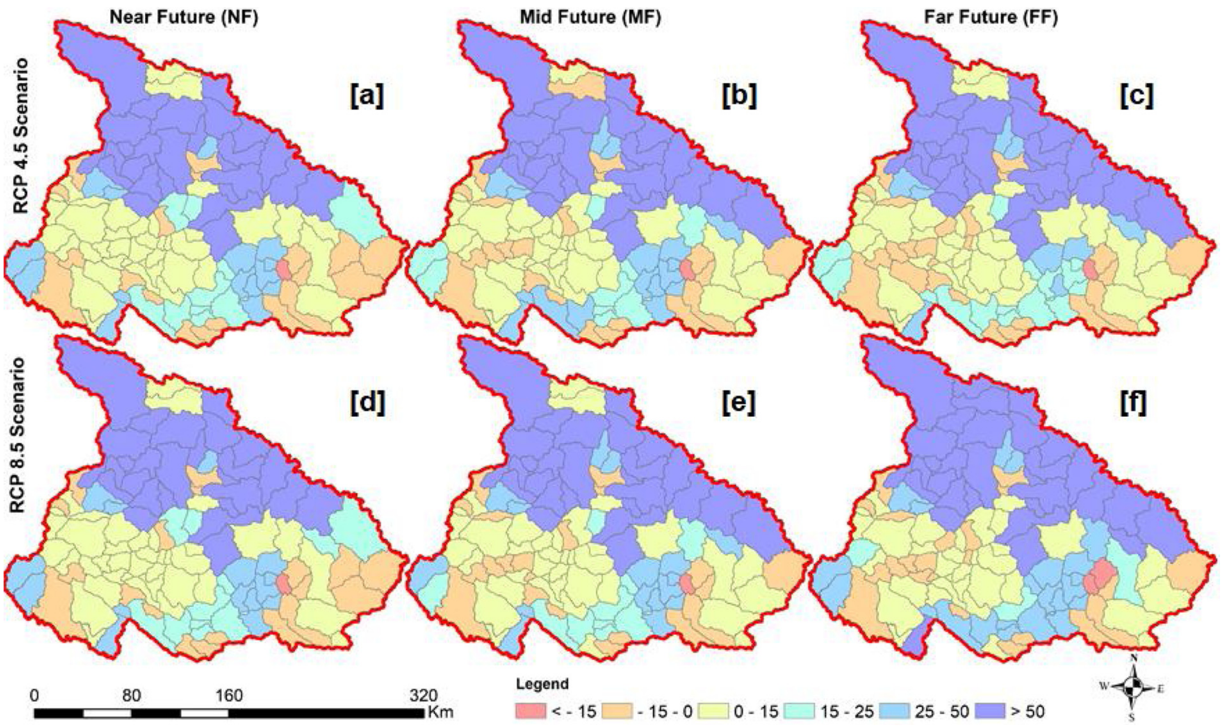

Fig. 6. Change (%) in average annual actual evapotranspiration with respect to the baseline.

decrease during pre-monsoon and monsoon seasons but increase in post-monsoon and winter seasons (January, November and December). The decrease during pre-monsoon and monsoon seasons are linked both to overall decrease in precipitation (though there are mixed trends, both increase and decrease, for different sub-basins of Bheri) (Fig. 5) and increase in AET as we move farther in the

Table 1

Percentage (%) of the sub-basins experiencing various levels of changes under two future scenarios and three futures considered.

Description	RCP4.5			RCP8.5		
	NF	MF	FF	NF	MF	FF
Increase in P by > 1%	44	50	43	44	50	43
Increase in P by > 10 %	10	26	32	19	31	32
Decrease in P by > 1%	49	46	47	49	44	47
Decrease in P by > 10 %	15	12	12	15	12	12
Increase in AET by > 1%	74	74	71	73	72	72
Increase in AET by > 10 %	51	51	51	51	53	53
Decrease in AET by > 1%	17	15	18	17	12	17
Decrease in AET by > 10 %	3	3	4	3	3	4
Increase in Q by > 1%	31	39	42	39	44	36
Increase in Q by > 10 %	14	18	23	19	21	20
Decrease in Q by > 1%	61	55	50	56	51	56
Decrease in Q by > 10 %	28	23	23	27	22	34

The range of alteration of projected average annual flow as well as variation across the months at the outlets of Karnali-main and its key tributaries are tabulated in Table 2, the changes with respect to baseline are shown in Fig. 8, and discussed hereunder.

Table 2

Projected change [%] in river flow at the outlets of key tributaries of Karnali river.

		Jan	Feb	Mar	Apr	May	Jun	Jul	Aug	Sep	Oct	Nov	Dec	Annual
Q270 [Bheri Outlet]	Baseline (m^3/s)	110.4	97.5	92.8	106.1	146.8	279.4	804.9	1209.1	769.8	370.0	198.3	146.5	361.0
	RCP4.5-NF	10.0	−6.1	−10.7	−19.1	−30.0	−26.3	−9.6	−4.1	0.4	−0.8	5.4	4.5	−5.4
	RCP4.5-MF	26.2	0.3	−6.2	−4.5	−11.0	1.5	1.2	0.4	1.3	4.8	18.4	16.9	3.0
	RCP4.5-FF	13.4	−5.6	−11.2	−16.9	−28.5	−12.5	−3.1	2.2	3.0	0.5	8.8	7.4	−0.7
	RCP8.5-NF	11.7	−3.9	−9.6	−18.4	−30.5	−25.7	−5.0	−0.3	3.3	1.2	7.9	6.7	−2.5
	RCP8.5-MF	13.5	−4.1	−10.0	−17.2	−28.5	−21.5	−4.2	0.0	4.8	2.6	9.8	7.6	−1.3
	RCP8.5-FF	11.3	−8.1	−16.4	−19.3	−28.5	−18.9	−3.6	−2.4	2.5	−0.7	6.0	5.6	−3.1
Q260 [Seti Outlet]	Baseline (m^3/s)	79.3	76.6	77.7	89.6	122.4	260.9	724.5	871.5	634.8	249.4	121.1	95.4	283.6
	RCP4.5-NF	57.3	28.9	32.5	40.5	28.2	7.9	4.5	12.0	4.8	18.2	29.2	35.6	13.9
	RCP4.5-MF	42.9	19.4	32.4	82.4	33.0	19.9	8.1	10.0	1.3	7.2	7.1	28.0	13.8
	RCP4.5-FF	46.0	16.7	27.2	29.8	20.5	5.7	10.8	18.1	9.6	22.2	29.8	30.3	16.1
	RCP8.5-NF	53.9	29.5	32.3	40.1	27.7	6.3	5.1	12.1	6.8	21.1	31.7	36.3	14.5
	RCP8.5-MF	41.4	20.6	29.5	33.2	22.3	8.9	9.3	17.7	7.5	23.7	30.1	30.6	16.0
	RCP8.5-FF	39.5	11.2	19.6	15.1	7.8	1.5	9.1	17.1	9.8	20.7	24.3	24.7	13.2
Q215 [Upper Karnal]	Baseline (m^3/s)	83.5	74.7	80.0	124.9	284.6	445.5	662.9	750.8	460.4	221.1	133.4	100.0	285.2
	RCP4.5-NF	20.5	12.8	21.6	43.6	−16.3	−31.2	−7.0	−8.3	−9.4	−3.0	−2.8	9.9	−7.3
	RCP4.5-MF	37.0	15.1	48.8	72.0	−6.0	−24.5	2.3	2.4	−7.7	0.4	9.5	58.2	2.3
	RCP4.5-FF	27.7	14.8	34.3	45.0	−12.1	−23.7	0.4	0.0	−10.3	0.6	8.9	47.0	−1.0
	RCP8.5-NF	19.9	13.7	23.6	40.8	−16.6	−30.2	−6.7	−8.2	−9.5	−2.7	−2.4	10.1	−7.2
	RCP8.5-MF	27.9	17.6	41.1	48.3	−12.3	−26.8	1.8	1.6	−9.2	−2.2	6.3	59.1	−0.3
	RCP8.5-FF	26.5	17.4	51.2	27.2	−22.9	−33.8	−3.7	−3.2	−13.8	−4.3	3.7	45.7	−5.8
Q220 [Tila Outlet]	Baseline (m^3/s)	18.0	15.2	14.7	18.5	27.1	40.9	85.7	126.0	98.2	60.1	32.1	23.0	46.6
	RCP4.5-NF	−12.9	−22.9	−25.5	−25.0	−25.8	−35.1	−14.9	−17.9	−19.2	−28.1	−24.3	−24.8	−21.6
	RCP4.5-MF	24.2	6.3	30.8	33.6	21.0	−5.9	7.2	−13.3	−13.5	−3.4	−2.2	−14.8	−1.2
	RCP4.5-FF	−7.7	−24.8	−19.8	−22.1	−20.9	−32.1	−0.7	−5.6	−12.2	−20.7	−15.0	−18.1	−13.4
	RCP8.5-NF	−11.2	−20.2	−24.0	−20.1	−22.6	−34.3	−11.7	−16.6	−18.0	−25.5	−20.7	−22.5	−19.5
	RCP8.5-MF	−12.2	−21.6	−20.6	−20.7	−22.3	−31.5	−3.9	−14.0	−15.7	−24.5	−20.9	−21.0	−17.2
	RCP8.5-FF	−7.3	−26.2	−25.2	−26.5	−20.1	−29.6	2.9	−8.1	−11.4	−18.2	−14.4	−16.9	−13.2
Q280 [Karnali-main]	Baseline (m^3/s)	350.7	301.8	301.3	428.0	791.6	1462.8	3253.3	4551.5	2960.1	1391.4	705.4	474.0	1414.3
	RCP4.5-NF	25.2	7.8	10.0	18.3	−1.9	−12.9	−0.8	−0.1	1.5	−2.7	7.1	10.3	0.6
	RCP4.5-MF	36.1	7.8	21.5	47.3	10.8	−0.3	6.7	3.3	1.4	−1.3	13.3	19.8	6.4
	RCP4.5-FF	28.7	2.9	12.0	17.7	−2.0	−9.2	5.2	5.4	3.4	−0.1	12.2	13.5	4.2
	RCP8.5-NF	25.0	8.8	10.9	18.1	−2.2	−12.7	1.2	1.4	3.3	−1.0	9.2	11.7	1.9
	RCP8.5-MF	27.0	5.0	14.5	19.7	−1.2	−10.6	4.7	5.0	3.9	−0.1	11.5	15.2	4.2
	RCP8.5-FF	26.1	0.7	11.4	8.6	−8.6	−14.9	3.5	2.5	2.8	−1.5	8.8	11.0	1.6

future, as evident from Fig. 6. However, projected increase in river flows during post-monsoon and winter seasons are likely due to contribution from the melting of snows and ice that are covering the headwaters of the Bheri river basin (please refer Pandey et al. (2020) for the land use/cover map). At least a quarter of the watershed area of Thuli Bheri (above Q265, please refer Fig. 1 for

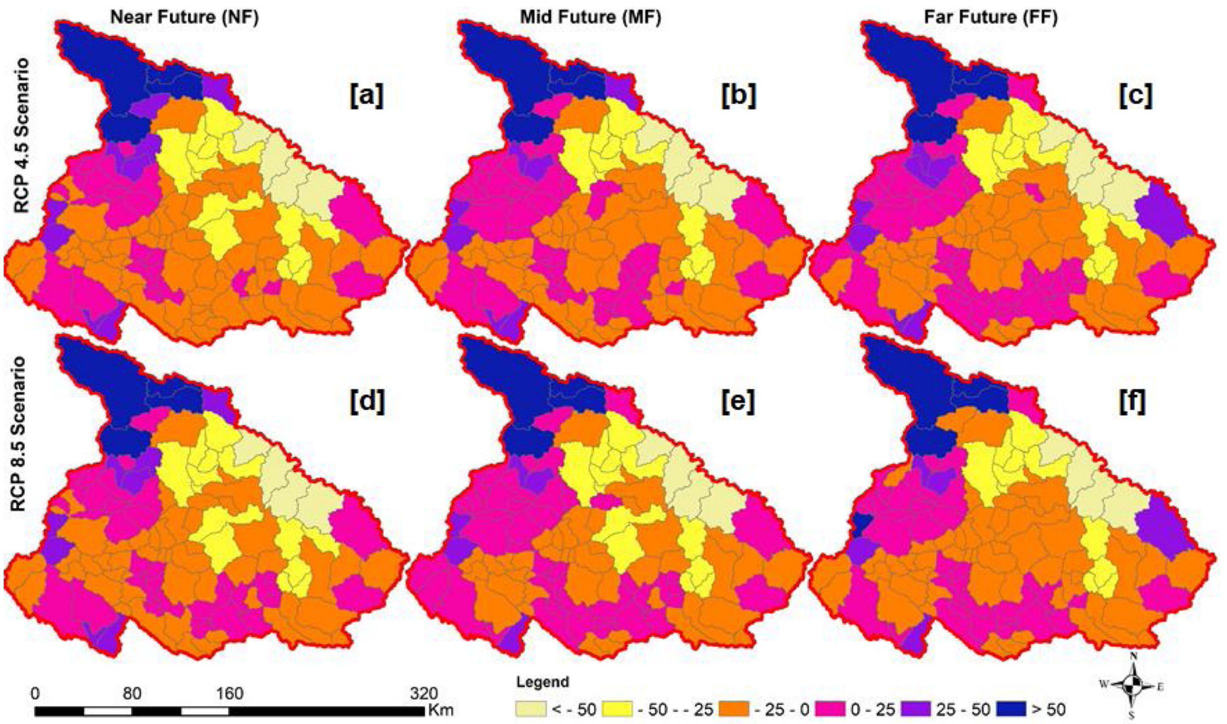

Fig. 7. Change (%) in average annual flows with respect to the baseline.

location) is covered with permanent snow and ice. Furthermore, percolation of monsoon season precipitation to aquifers and appearing that into the river in the form of baseflow could also have contributed to increase in the river flows in the post-monsoon and winter seasons.

4.2. Seti river basin

The Seti river basin above Q260 hydrological station covers an area of 7460 km^2. The average annual flow volume at Q260 for the baseline period is estimated at 8944 MCM, which under RCP4.5 scenarios is projected to increase from 13.9 % in NF to 16.1 % in FF. In case of RCP8.5 scenarios, it is projected to increase from 14.5 % in NF to 16.0 % in MF. The rate of increase, however, is not consistent across the months, scenarios, and future periods considered. The projected changes in monthly flow volumes under both the scenarios vary from 4.5 % (July) to 57.3 % (January) in NF, 1.3 % (September) to 82.4 % (April) in MF, and 1.5 % (June) to 46.0 % (January) in FF. The flow volumes in the Seti river is projected to increase across all the months, albeit with varying rates; higher increase in winter, pre-monsoon and post-monsoon seasons and lower during the monsoon season. The increase in flow volume in the Seti river outlet is likely due to increase in precipitation in the basin (Fig. 5) and varying rates across the seasons are due to varying amount of precipitation and actual evapotranspiration. Therefore, future water infrastructure projects such as hydropower and irrigation have potential to get benefited from more water availability during dry seasons.

4.3. Upper Karnali river basin

The Upper Karnali river basin in this study refers to the area above Q215 hydrological station. It covers an area of 15,200 km^2. The average annual flow volume at Q215 is estimated at 8993 MCM, which is projected to change by -7.3 % in NF and 2.3 % in MF. Under the RCP8.5 scenarios, the projected changes are -7.2 % in NF and -5.8 in FF. The projected changes are not uniform throughout the months, which vary from -31.2 % (June) to 43.6 % (April) in NF, -26.8 % (June) to 72 % (April) in MF, and -33.8 % (June) to 51.2 % (March) in FF. The flow volumes are projected to decrease during monsoon season (JJAS) and increase during winter and pre-monsoon season; albeit with varying rates. Both decrease in precipitation and increase in AET are projected for the sub-basins in the Upper Karnali river basin (Figs. 5 and 6) thus resulting in decrease in flows during monsoon season. However, given the large area of the Upper Karnali river basin covered with permanent snow and ice, melting of snow and ice contributes to increase in river flows during pre-monsoon and winter seasons.

4.4. Tila river basin

The Tila river basin here refers to the area above Q220 hydrological station. It covers an area of 1870 km^2. The average annual

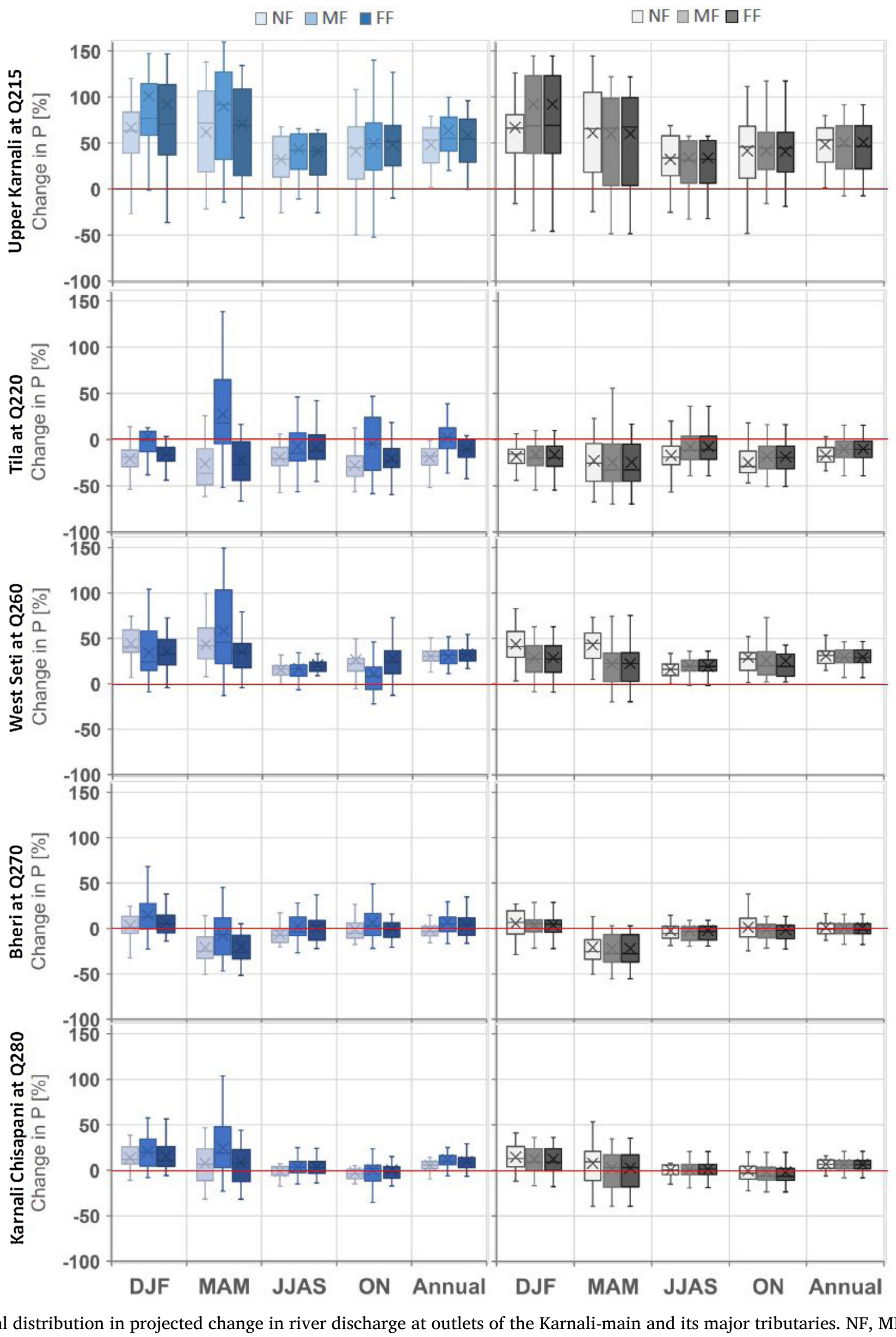

Fig. 8. Temporal distribution in projected change in river discharge at outlets of the Karnali-main and its major tributaries. NF, MF and FF refer to Near-, Mid-, and Far-Futures, respectively. Each box represents range in each season, whiskers indicate max and min values excluding the outliers, '-' marker indicate median, and 'x' marker indicate mean.

flow volume at Q220 is estimated at 1470 MCM, which under RCP4.5 scenarios is projected to change by -21.6 % in NF and -13.4 % in FF. Under the RCP8.5 scenarios, it is projected to alter by -19.5 % in NF, -17.2 % in MF, and -13.2 % in FF. The intra-annual variations across the months are -35.1 % (June) to -11.2 % (January) in NF, -31.5 % (June) to 33.6 % (April) in MF, and -32.1 % (June) to 2.9 % (July) in FF. Except in March and April in MF under RCP4.5, projections for all other scenarios and futures show decrease in flow volume across all the months/seasons, it is because sub-basins of Tila also shows projected decrease in precipitation (Fig. 5) and increase in actual evapotranspiration (Fig. 6).

4.5. Karnali-main river basin

The Karnali-main river basin here refers to the area above Q280 hydrological station. It covers an area of 42,890 km^2. The average annual flow volume near to the outlet of Karnali-main (before joining Mohana) [at Q280 station] for the baseline period is estimated at 44,602 MCM, which in NF and MF are projected to increase by only 0.6 % and 6.4 % under RCP4.5 and 9% and 4.2 % under RCP8.5 scenarios, respectively. The projections, however, varies across the months for different scenarios and future periods. For example, projected changes under both the scenarios in NF vary from -12.9 % (June) to 25.2 % (January). When moving towards mid-future, it varies from -10.6 % (June) to 47.3 % (April); and in far-future it ranges from -14.9 % (June) to 28.7 % (January). Future flow volume is projected to decrease in June and increase winter and later stage of the monsoon season even though the average annual is projected to increase. As the KarMo is the snow-fed river basins, increase in river flows from the later stage of the monsoon to winter are potentially the contributions from melting of snow and ice.

5. Conclusions

This study applied a well calibrated and validated SWAT hydrological model to assess impacts of climate change on spatio-temporal distribution of water availability in the Karnali-Mohana (KarMo) basin located in Western Nepal. Future climate was projected based on an ensemble of selected RCMs for six consensus cases from a set of 19. The temperature (T) is projected to have an increasing trend across all regions and seasons, with highest amount of increase for the mountain stations in the winter season. The amount of increase in the projections vary across the seasons, however, no strong skewness suggests annual values can represent a seasonal change in the region. Projection in the minimum temperature also follows similar spatio-temporal trends across the stations. In case of projected precipitation, it does not have a distinct spatio-temporal trend at the seasonal or annual scale. The highest variability in total P is seen for the post-monsoon season (ON), especially for the mountains and hills, indicating wetter dry seasons for future. With both maximum T and P increasing on an average in the winter seasons, glacier and snow-melt may be expected to increase.

The impacts of projected change in climate to spatio-temporal distribution of water availability was assessed by perturbing the climatic inputs to the calibrated/validated SWAT model with projected future time-series of P and T. As a result of changes in P, T and AET, average annual flow at outlets of the KarMo sub-basins are projected to alter, however, in general, following similar patterns as P. The impacts in the sub-basins at higher altitudes are relatively higher, indicating higher vulnerability to CC of the high mountain regions of the basin than the flat lands in Tarai. For example, in NF under RCP4.5 scenarios, the annual flow volume at the outlet of Tila is projected to change by -21.6 %, at upper Karnali by -7.2 %, Seti by +13.9 %, Bheri by -5.4 %, and Karnali-main by 0.6 %. It clearly reflects the spatial-heterogeneity in the impacts of projected CC on an annual scale. In addition, projected alterations also vary across the seasons. Taking the case of RCP4.5 and NF again, it alters from -35.1 % (June) to -11.2 % (January) in Tila, -31.2 % (June) to 43.6 % (April) in upper Karnali, 4.5 % (July) to 57.3 % (January) in Seti, -30.5 % (May) to 11.7 % (January) in Bheri, and -12.9 % (June) to 25.2 % (January) in Karnali-Main.

These findings from this study are valuable information for water resources planners and managers for developing location-specific strategies even within a single basin for sustainable utilization of water resources for the country's prosperity.

Authorship contribution

Vishnu: Overall structuring of the contents, conceptualizing flow of contents, drafting methodology, and results/discussion as well as conclusion sections, and coordinate with co-authors, and managing references, tables, figures.

Sanita: Climate data pre-processing, future climate projection, developing draft of contents related to climate projection; feedback/input on improving the draft of entire contents.

Luna: Contribution in conceptualization of contents, overall guidance, review and feedback/input for improving overall quality of the entire manuscript.

Bhesh: Contribution in visualizing overall scope of the manuscript, drafting of introduction section, feedback/input on improving the draft of entire contents.

Declaration of Competing Interest

The authors declare that they have no known competing financial interests or personal relationships that could have appeared to influence the work reported in this paper.

Acknowledgements

This study is made possible by the generous support of the American people through the United States Agency for International Development (USAID) under Digo Jal Bikas (DJB) projected. The contents are the responsibility of the authors and do not necessarily reflect the views of USAID or the United States Government.

Appendix A. Supplementary data

Supplementary material related to this article can be found, in the online version, at doi:https://doi.org/10.1016/j.ejrh.2020.100691.

References

Abbaspour, K.C., Faramarzi, M., Ghasemi, S.S., Yang, H., 2009. Assessing the impact of climate change on water resources in Iran. Water Resour. Res. 45 (10), 1–16.
Arnold, J.G., Srinivasan, P., Muttiah, R.S., Williams, J.R., 1998. Large area hydrologic modelling and assessment. Part I. Model development. J. Am. Water Resour. Assoc. 34, 73–89.
Aryal, A., Shrestha, S., Babel, M.S., 2018. Quantifying uncertainty sources in an ensemble of hydrological climate impact projections. Theor. Appl. Climatol. 135, 193–209. https://doi.org/10.1007/s00704-017-2359-3.
Bajracharya, A.R., Bajracharya, S.R., Shrestha, A.B., Maharjan, S.B., 2018. Climate change impact assessment on the hydrological regime of the Kaligandaki Basin, Nepal. Sci. Total Environ. 625, 837–848.
Bastola, S., Murphy, C., Sweeney, J., 2011. The role of hydrological modelling uncertainties in climate change impact assessments of Irish river catchments. Adv. Water Resour. 34 (5), 562–576. https://doi.org/10.1016/j.advwatres.2011.01.008.
Bates, B.C., Kundzewicz, Z.W., Wu, S., Palutikof, J.P., 2008. Climate Change and Water. https://doi.org/10.1016/j.jmb.2010.08.039.
Berg, P., Feldmann, H., Panitz, H.J., 2012. Bias correction of high resolution regional climate model data. J. Hydrol. 448–449, 80–92.
Bharati, L., Gurung, P., Jayakody, P., Smakhtin, V., Bhattarai, U., 2014. The projected impact of climate change on water availability and development in the Koshi Basin, Nepal. Res. Dev. 34, 118–130.
Bharati, L., Gurung, P., Maharjan, L., Bhattarai, U., 2016. Past and future variability in the hydrological regime of the Koshi Basin, Nepal. Hydrol. Sci. J. 61 (1), 79–93.
Choudhary, A., Dimri, A.P., 2018. Assessment of CORDEX-South Asia experiments for monsoonal precipitation over the Himalayan region for future climate. Clim. Dyn. 50 (7–8), 3009–3030.
Clarke, J.M., Whetton, P.H., Hennessy, K.J., 2011. Providing application-specific climate projections datasets: CSIRO's climate futures framework. MODSIM2011. 19th Int. Congr. Model. Simul. 2683–2687. https://doi.org/10.13140/2.1.1915.2649.
Devkota, L.P., Gyawali, D.R., 2015. Impacts of climate change on hydrological regime and water resources management of the Koshi River Basin, Nepal. J. Hydrol. Reg. Stud. 4, 502–515. https://doi.org/10.1016/j.ejrh.2015.06.023.
Dhami, B., Himanshu, S.K., Pandey, A., Gautam, A.K., 2019. Evaluation of the SWAT model for water balance study of a mountainous snowfed river basin of Nepal. Environ. Earth Sci. 77, 21.
Dhaubanjar, S., Pandey, V.P., Bharati, L., 2019. Climate futures for Western Nepal based on regional climate models in the CORDEX-SA. Int. J. Climatol. 40 (4), 2201–2225. https://doi.org/10.1002/joc.6327.
Gudmundsson, L., Bremnes, J.B., Haugen, J.E., Engen-Skaugen, T., 2012. Technical Note: downscaling RCM precipitation to the station scale using statistical transformations – a comparison of methods. Hydrol. Earth Syst. Sci. 16 (9), 3383–3390.
Honti, M., Scheidegger, A., Stamm, C., 2014. Importance of hydrological uncertainty assessment methods in climate change impact studies. Hydrol. Earth Syst. Sci. Discuss. 11 (1), 501–553. https://doi.org/10.5194/hessd-11-501-2014.
IPCC, 2014. In: Pachauri, R.K., Meyer, L.A. (Eds.), Climate Change 2014: Synthesis Report. Contribution of Working Groups I, II and III to the Fifth Assessment Report of the Intergovernmental Panel on Climate Change. Core Writing Team. https://doi.org/10.1017/CBO9781107415324.004.
Kundzewicz, Z.W., Mata, L.J., Arnell, N.W., Döll, P., Jimenez, B., Oki, T., et al., 2009. The implications of projected climate change for freshwater resources and their management resources and their management. Hydrol. Sci. J. 6667 (January), 2–10.
Lutz, A.F., ter Maat, H.W., Biemans, H., et al., 2016. Selecting representative climate models for climate change impact studies: an advanced envelope-based selection approach. Int. J. Climatol. 36, 3988–4005. https://doi.org/10.1002/joc.4608.
Maraun, D., 2014. Bias correction, quantile mapping, and downscaling: revisiting the inflation issue. J. Clim. 26 (2013), 2013–2014.
Pandey, V.P., Dhaubanjar, S., Bharati, L., Thapa, B.R., 2019. Hydrological response of Chamelia watershed in Mahakali Basin to climate change. Sci. Total Environ. 650 (Part 1), 365–383.
Pandey, V.P., Dhaubanjar, S., Bharati, L., Thapa, B.R., 2020. Spato-temporal distribution of water availability in Karnali-Mohana Basin, Western Nepal: Hydrological model development using multi-site calibration approach (Part-A). J. Hydrol.– Reg. Stud EJRH_100690, In press.
Sanjay, J., Krishnan, R., Shrestha, A.B., et al., 2017. Downscaled climate change projections for the Hindu Kush Himalayan region using CORDEX South Asia regional climate models. Adv. Clim. Change Res. 8, 185–198.
Shrestha, S., Shrestha, M., Babel, M.S., 2016. Modelling the potential impacts of climate change on hydrology and water resources in the Indrawati River Basin, Nepal. Environ. Earth Sci. 75 (4), 1–13. https://doi.org/10.1007/s12665-015-5150-8.
Shrestha, M., Acharya, S.C., Shrestha, P.K., 2017. Bias correction of climate models for hydrological modelling – are simple methods still useful? Meteorol. Appl. 24 (3), 531–539.
Stonefelt, M.D., Fontaine, T.A., Hotchkiss, R.H., 2000. Impacts of climate change on water yield in the upper Wind River basin. J. Am. Water Resour. Assoc. 36 (2), 321–336.
Talchabhadel, R., Karki, R., Thapa, B.R., Maharjan, M., 2018. Spatio-temporal variability of Extreme precipitation in nepal. Int. J. Climatol. 38 (11), 4296–4313. https://doi.org/10.1002/joc.5669.
Teutschbein, C., Seibert, J., 2010. Regional climate models for hydrological impact studies at the catchment scale: a review of recent modeling strategies: regional climate models for hydrological impact studies. Geogr. Compass 7, 834–860.
Trang, N.T.T., Shrestha, S., Shrestha, M., Datta, A., Kawasaki, A., 2017. Evaluating the impacts of climate and land-use change on the hydrology and nutrient yield in a transboundary river basin: a case study in the 3S River Basin (Sekong, Sesan, and Srepok). Sci. Total Environ. 576, 586–598.
UN-WWAP, 2015. World Water Development Report 2015: Water for a Sustainable World. The United Nations World Water Assessment Program (UN-WWAP). UNESCO, Paris.
WECS, 2011. Water Resources of Nepal in the Context of Climate Change. Water and Energy Commission Secretariat (WECS), Government of Nepal, Kathmandu.
Whetton, P., Hennessy, K., Clarke, J., McInnes, K., Kent, D., 2012. Use of Representative Climate Futures in impact and adaptation assessment. Clim. Change 115, 433–442.
Zhu, T., Ringler, C., 2012. Climate change impacts on water availability and use in the Limpopo river basin. Water 4, 63–84.